Proceedings of the 16th International Conference on Soil Mechanics and Geotechnical Engineering

doi:10.3233/978-1-61499-656-9-429

Mechanical behaviour for granular soils using the Principle of Natural Proportionality, undrained case

Comportement mécanique des sols pulvérulents utilisant le Principe de la Proporcionnalité Naturelle en conditions non drainées

Rigoberto Rivera-Constantino & Eulalio Juárez-Badillo
Graduate School of Engineering, National University of Mexico
Felipe de Jesús Jerónimo-Rodríguez
School of Civil Engineering, Universidad Michoacana de San Nicolás de Hidalgo

ABSTRACT
The Principle of Natural Proportionality (PNP) postulated in 1985 is a unifying principle from which many general equations used to describe the mechanical behaviour of geomaterials have emerged. This time improved general equations obtained by the PNP were applied to describe the stress-strain and pore pressure behavior for granular soils (sands) tested in undrained triaxial compression tests between confining pressures 50 kPa and 500 kPa. The stress-strain behaviour was fitted using the pre-peak inverted function and the post-peak ductility function. The general equation for pore pressure given by the PNP was also applied to describe the pore pressure behaviour all along the triaxial tests. The different stress-strain and pore pressure parameters that describe the behaviour of granular soils are reported.

RÉSUMÉ
Le Principe de la Proportionnalité Naturelle a été développé en 1985, il est un Principe unificateur qui a fournit des plusieurs équations générales utilisées en la description mécanique des geo-matériaux. Actuellement les équations générales du comportement obtenues du Principle de la Proportionnalité Naturelle ont été améliorées et cette fois ci, elles ont été appliquées aux sables soumis à des essais triaxiaux non drainés, ce qui a permet de faire une description des résultats expérimentaux concernant les curbes contrainte-déformation et pression interstitielle, dans un intervalle de pressions de confinement entre 50 kPa et 500 kPa. La prédiction du comportement contrainte-déformation pour des contraintes inférieures au pic atteint a été faite en utilisant la fonction inversée tandis que pour des contraintes supérieures au pic atteint nous avons utilisé la fonction de ductilité. Pou faire la prédiction de la pression interstitielle produit pendant l'application du déviateur de contrainte (q) nous avons utilisé une seule équation générale pour tout l´essai. Les différents paramètres utilisés dans les équations générales du comportement ont été rapportés.

1 INTRODUCTION

The PNP establishes that all natural phenomena are susceptible of being described in an ordered and simple manner using proper variables and their corresponding proper functions with complete domain, zero to infinite (Juárez-Badillo 1985).

This Principle that constitutes a quite different way to establish constitutive equations for geomaterials, has been successfully applied by the second author to soils, rocks, concrete, ice and fluids. In the case of sands, the general equations for stress-strain, volume changes and pore pressures have been applied by the second author in an isolated manner (Juárez-Badillo 1997, 1999a, 1999b 1999c), not permitting get conclusive results.

Some experimental results related to the undrained compressive behaviour of granular soils are presented in this paper. These results belong to very complete study undertaken by the authors for the drained and undrained stress-strain behaviour of granular soils (Jerónimo-Rodríguez, 2003). The stress-strain and pore pressure behaviour for the granular soils were adjusted using the theoretical equations emerged from the PNP. To finish, the representative parameters of the granular soils studied are reported.

2 STRESS-STRAIN AND PORE PRESSURE EQUATIONS

The theoretical stress-strain equation applied are (Juárez-Badillo 1999a). The pre-peak inverted function y_I , Fig. 1

$$y_I = \frac{(\sigma_1 - \sigma_3)}{(\sigma_1 - \sigma_3)^*} = \left[\frac{e_{af}}{e_a} - 1 \right]^{-\frac{1}{\nu}} \quad (1)$$

where:

e_a: axial deviatoric natural strain, negative in triaxial compression tests
e_{af}: final e_a at $\sigma=\infty$
ν: shear coefficient
$(\sigma_1-\sigma_3)$: deviator stress
$(\sigma_1-\sigma_3)^*$= characteristic $(\sigma_1-\sigma_3)$ at $e_a=1/2\ e_{af}$
σ_1 y σ_3: mayor and minor principal stresses, respectively

Eq. (1) may be written as:

$$\frac{e_a}{e_{af}} = \left[1 + \left(\frac{(\sigma_1 - \sigma_3)}{(\sigma_1 - \sigma_3)^*} \right)^{-\nu} \right]^{-1} \quad (2)$$

The equation used for the post-peak region is

$$\frac{e_a}{e_{a1}} = \left[\frac{x - x_\infty}{x_1 - x_\infty} \right]^{-\nu} \quad (3)$$

where:
$x=(\sigma_1-\sigma_3/\sigma_{co})$: normalized deviatoric stress
σ_{co}: initial consolidation stress
(e_{a1}, x_1): known point in the post-peak region
$x_\infty=x$ for $e_a=\infty$ for the post-peak region

The Eq. (3) is known as post-peak ductility function y_D, Fig. 2, and may be written as a function of $(\sigma_1-\sigma_3)$ as:

$$(\sigma_1-\sigma_3)=(\sigma_1-\sigma_3)_\infty+\left[(\sigma_1-\sigma_3)_1-(\sigma_1-\sigma_3)_\infty\right]\left[\frac{e_a}{e_{a1}}\right]^{-\frac{1}{\nu}} \quad (4)$$

The theoretical pore pressure equation provided by the PNP in its complete form is:

$$\Delta u=\Delta\sigma_i+\alpha\sigma_{co}\frac{\sigma_{co}}{\sigma_{eo}}y-\alpha_e(\sigma_{eo}-\sigma_{co})y_e \quad (5)$$

where:
$\Delta\sigma_i$: isotropic stress increment
σ_{eo}: initial equivalent consolidation pressure due to the interlocking of solid particles $\sigma_{eo}\geq\sigma_{co}$
y: sensitivity function given by Ec. (6), Fig. 3

$$y=\left[1+\left(\frac{e_a}{e_a^*}\right)^{-\beta}\right]^{-1} \quad (6)$$

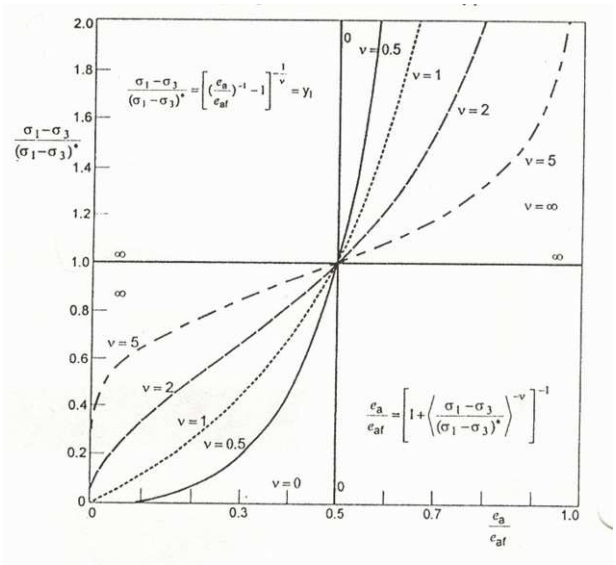

Fig. 1. Graphs of the pre-peak inverted function y_I

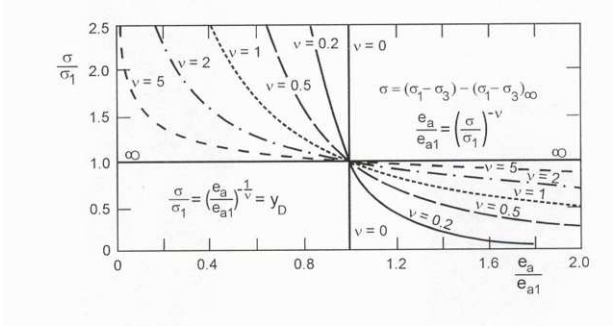

Fig. 2. Graphs of the post-peak ductility function y_D

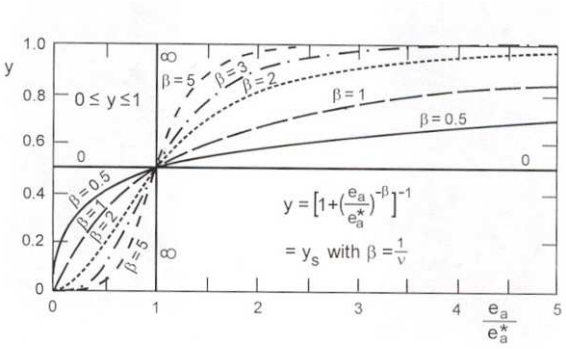

Fig. 3. Graphs of the sensibility function y

In this equation $e_a^*=e_a$ at y=1/2 and α y β are pore pressure parameters where $\alpha\leq1$. The susbcript e in α y β in the last term of Eq. (5) is only to distinguish them from the coefficients in the second term. Obseve that the second and the third terms in Eq. (5) are a compresive term due to σ_{co} and a dilatant term due to interlocking. In many triaxial tests has been found that $\alpha_e=\alpha$ and $y_e=y$ and therefore Eq. (5) may be written as:

$$\Delta u=\Delta\sigma_i+\alpha\left[\sigma_{co}\frac{\sigma_{co}}{\sigma_{eo}}-\left(\sigma_{eo}-\sigma_{co}\right)\right]y \quad (7)$$

Observe that the term α is iqual zero if $\sigma_{eo}/\sigma_{co}=1.618$ and that is positive if $\sigma_{eo}/\sigma_{co}<1.618$ and it is negative if $\sigma_{eo}/\sigma_{co}>1.618$.

3 CHARACTERISTIC OF SAMPLES AND TESTING PROCEDURE

3.1 *Soil testing*

Soil material tested was standard sand (Ottawa sand 20-30). The particles consisting of quartz are sub-rounded.

The soil particles are poorly graded, and the coefficients of uniformity (C_u) and curvature (C_c) are 1.2 and 1.0, respectively. The effective and mean diameters D_{10} and D_{50} are 0.63 and 0.70, respectively. The specific gravity is 2.65.

The maximum and minimum void ratios of the soil tested were 0.80 and 0.49.

3.2 *Testing procedure*

The soil specimens were prepared by wet tamping and air-pluviation. In the earlier case the soil was compacted in a mold in ten layers. Air-pluviation was used for the loose specimens. The specimen was fully saturated by using CO_2-gas and deaired water and isotropically consolidated applying effective stress between 100 kPa y 500 kPa. The back-pressure used was 300kPa for all tests. The Skempton´s B-value larger than 0.95 was measured in all tests.

The relative density values of the specimens were between 100 y 52%. In the instrumented triaxial device the specimen size was 36 mm diameter and 80 mm height. The soil specimen was loaded monotonically as a strain-control test, using a strain rate of 0.10 mm/min (Head, 1994). No effect of membrane penetration was considered during monotonic load due the mean diameter of the soil.

The index properties of specimens tested are reported in Table 1.

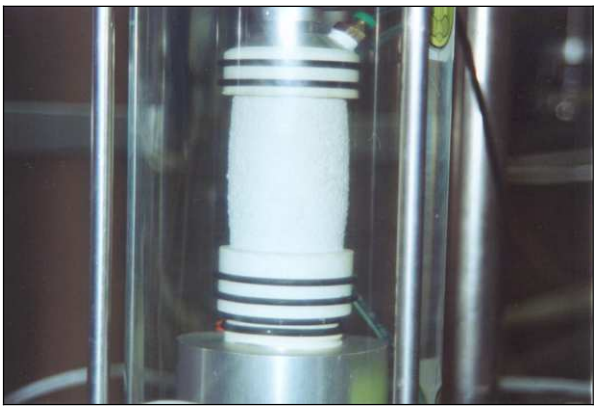

Fig. 4. Geometry of Ottawa sand specimen seen at e_a=-10%

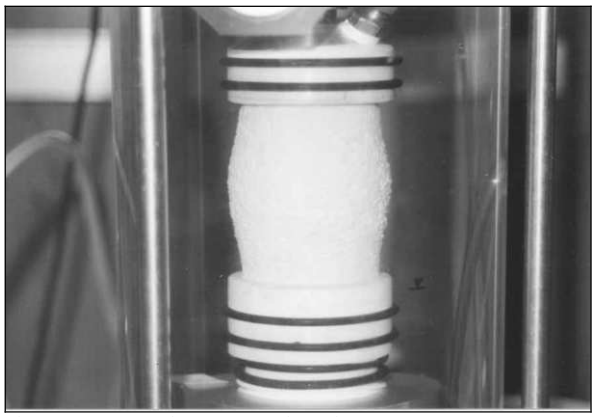

Fig. 5. Geometry of Ottawa sand specimen seen at e_a=-25%

Table 1. Index and mechanical properties of the specimen tested

Serie	Test	e	Dr (%)	σ_{co} kPa	q_{peak} kPa	M_{peak}	ϕ_{peak} (°)	ϕ_{∞} (°)	E_s kPa
	A7	0.64	52	100	660	1.06	27	19	4656
UCT-4	A8	0.64	52	300	1056	1.17	29	25	10309
	A9	0.64	52	500	1557	1.22	31	23	32508
	A10	0.58	71	100	727	1.15	29	15	8253
UCT-6	A11	0.60	65	300	1253	1.22	31	19	15416
	A12	0.61	61	500	1778	1.25	31	25	34871
	A4	0.53	87	100	1062	1.34	33	19	14309
UCT-2	A5	0.54	84	300	1425	1.33	33	26	20227
	A6	0.54	84	500	1923	1.34	33	27	33669
UCT-1	A3	0.49	100	500	1996	1.37	34	25	29505

Table 2. Parameters values in the natural proportionality stress-strain and pore pressure equations

		Stress-strain							Pore pressure					
No.	Test	Pre-Peak, Eq. (2)			Post-Peak, Eq. (4)				Eq. (7)					
Serie	No.	ν	e_{af}	$(\sigma_1-\sigma_3)^*$	ν	e_{a1}	$(\sigma_1-\sigma_3)_1$	$(\sigma_1-\sigma_3)_\infty$	σ'_{co}	σ_{co}	σ_{co}/σ'_{co}	α	β	e_{a^*}
	A7	2	-0.200	440	1	-0.20	664	455	100	625	6.3	1.00	2	-0.096
UCT-4	A8	2.5	-0.250	925	1	-0.20	1140	842	300	945	3.2	1.00	3	-0.080
	A9	2	-0.250	2250	1	-0.20	1830	958	500	1279	2.6	1.00	2	-0.039
	A10	2	-0.070	280	1	-0.20	660	308	100	547	5.5	1.00	2	-0.050
UCT-6	A11	2.5	-0.070	520	1	-0.20	1130	615	300	932	3.1	1.00	3	-0.049
	A12	2	-0.090	1440	1	-0.20	1730	1240	500	1432	2.9	1.00	3	-0.029
	A4	2	-0.050	300	1	-0.20	1080	445	100	612	6.1	1.00	3	-0.033
UCT-2	A5	2	-0.070	700	1	-0.20	1260	960	300	1029	3.4	1.00	3	-0.042
	A6	2	-0.065	1050	1	-0.20	1670	1358	500	1451	2.9	1.00	3	-0.035
UCT-1	A3	2.5	-0.070	980	1	-0.20	1660	1190	500	1382	2.8	1.00	4	-0.039

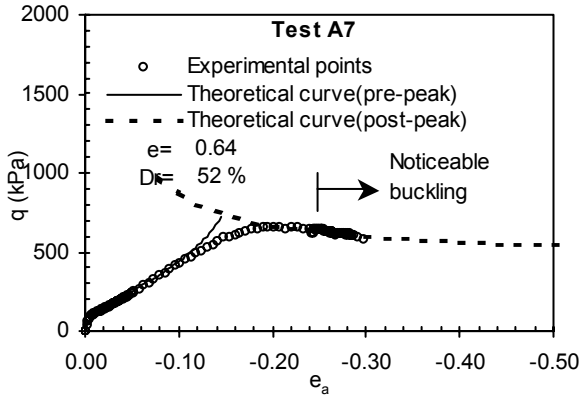

Fig. 6a. Stress-strain relationship, σ'_{co}=100 kPa.

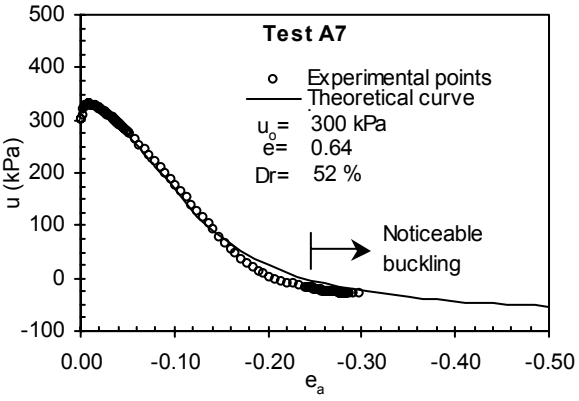

Fig. 6b. Pore pressure-strain relationship, σ'_{co}=100 kPa.

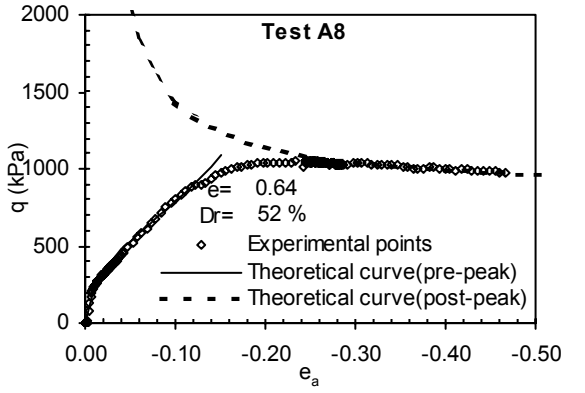

Fig. 7a. Stress-strain relationship, σ'_{co}=300 kPa.

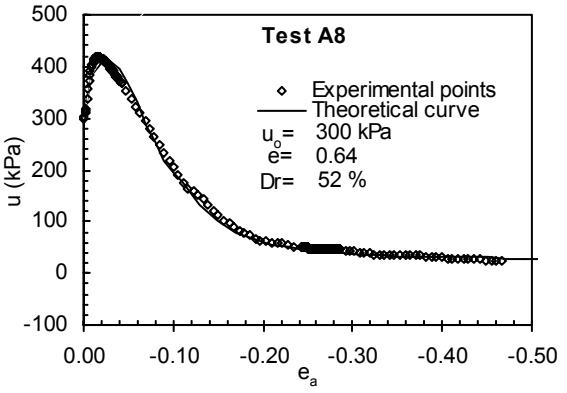

Fig. 7b. Pore pressure-strain relationship, σ'_{co}=300 kPa.

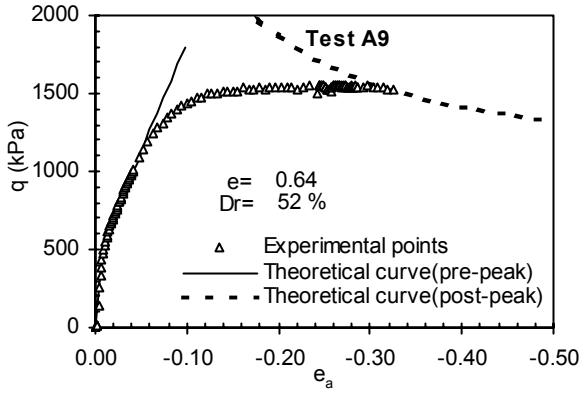

Fig. 8a. Stress-strain relationship, σ'_{co}=500 kPa.

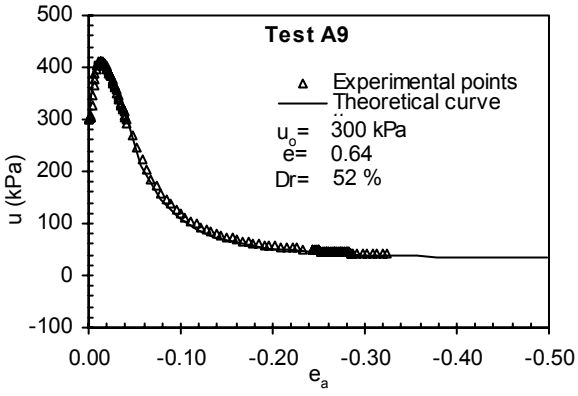

Fig. 8b. Pore pressure-strain relationship, σ'_{co}=500 kPa.

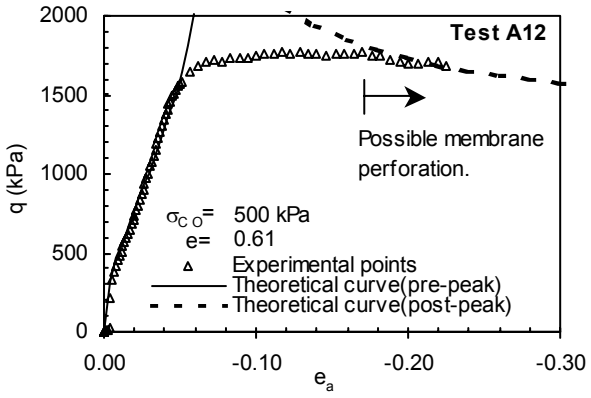

Fig. 9a. Stress-strain relationship, Dr=61 %.

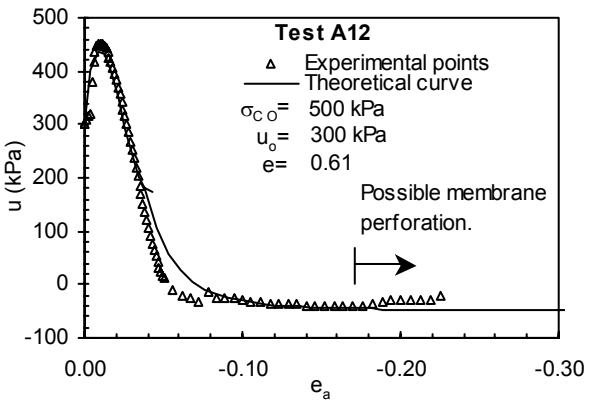

Fig. 9b. Pore pressure-strain relationship, Dr=61 %.

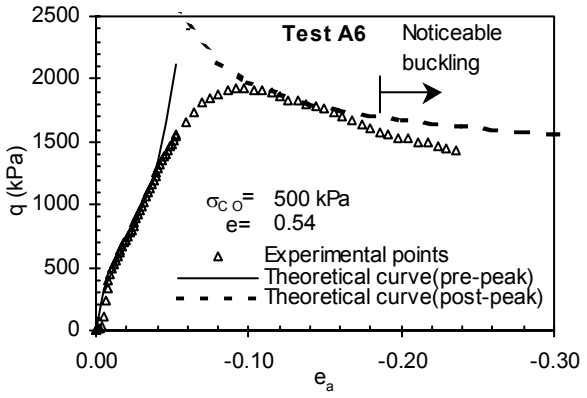

Fig. 10a. Stress-strain relationship, Dr=84 %.

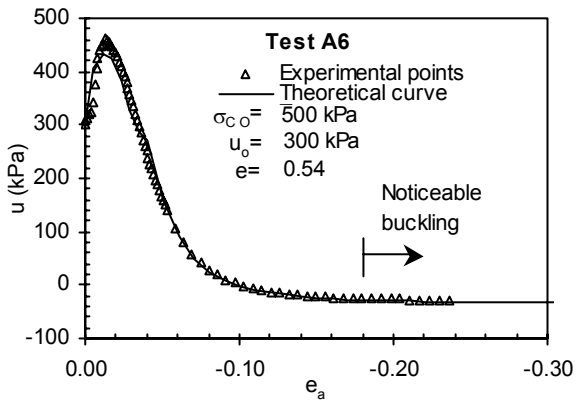

Fig. 10b. Pore pressure-strain relationship, Dr=84 %.

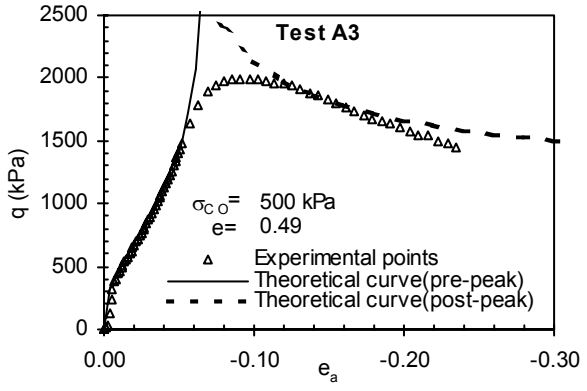

Fig. 11a. Stress-strain relationship, Dr=100 %.

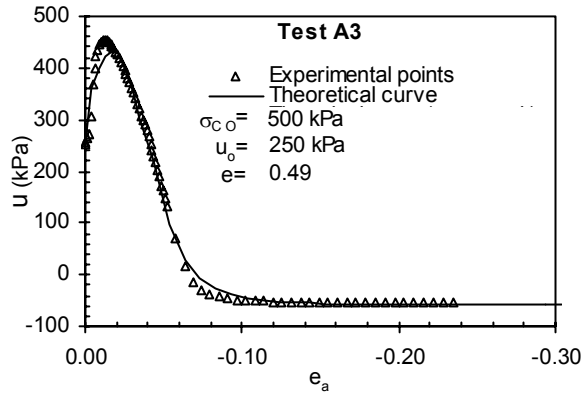

Fig. 11b. Pore pressure-strain relationship, Dr=100 %.

4 TEST RESULTS AND THEORETICAL ADJUST

The theoretical adjust for the sand tested was made for the curves stress-strain and pore pressure.

The geometry of the Ottawa sands specimens seen at -10 % and -25 % strain are presented in Figs. 4 and 5, respectively. It is clear that the stress and strain obtained as the average for the whole specimen volume, are not entire representative, because are inhomogeneous. Obviously, the post-peak region will be more affected by this phenomenon than the pre-peak region. This fact is not taken into account in the theoretical adjust.

Nevertheless the strain values lower than 25 % will be considered as homogeneous in this research.

Table 1 is a summary of the experimental results obtained in the triaxial tests. It contains a report of the maximum values of the deviator stress (q_{peak}), slope value in the space p-q (M_{peak}), maximum friction angle (ϕ_{peak}), residual friction angle (ϕ_∞) and secant modulus for the 50% q_{peak} (E_s).

Table 1 indicates that q_{peak} and E_s increase as the consolidation stress and the relative density increase too.

The parameters values in the theoretical equations used for the theoretical adjust of the strain-stress and pore pressure curves are reported in Table 2. The theoretical equations used were (2) and (4) for the strain-stress curves in the pre-peak (inverted function) and post-peak (ductility function) regions, respectively. The pore pressure description was made using the Eq. (7).

4.1 *Stress-strain behaviour*

Some experimental results related to stress-strain behaviour are presented in Figs. 6a to 11a as well as the theoretical adjust.

Figs. 6a to 8a are for a constant relative density and variable consolidation stress while Figs. 9b to 11b are for a constant consolidation stress and variable relative density. These figures show that the theoretical adjust is very satisfactory in the pre-peak and post-peak regions.

4.2 *Pore pressure-strain behaviour*

The experimental results for a constant relative density and different consolidation stress are reported in Figs. 6b to 8b, while for a constant consolidation stress and different relative density are shown in Figs. 9b to 11b.

These figures show that for the axial strain smaller than 2% the material present a contractive behaviour. The pore pressure increase as the strain increase too until a maximum value is attained.

Afterwards the pore pressure decreases until a minimum value is reached. This value is close to the maximum deviator stress. Some search found that when the negative pore pressure values are close to –100 kPa threshold the cavitation phenomena is presented (McManus and Davis, 1997, Ovando, 1985). In this search the lowest negative pore pressure values were –55 kPa, therefore non cavitation phenomena was found. The pore pressure was adjusted very satisfactory using the theoretical equation (7). It is important to observe that the pore pressure-strain description was made without taking into account the experimental isotropic stress decrease in the post peak region though it was important in many of the tests. In the post peak the isotropic component of the pore pressure was considered constant and equal to the isotropic component corresponding precisely to the peak. This point is very important and should be further studied in the future.

5 CONCLUSIONS

Undrained monotonic loading triaxial tests on Ottawa sand have been carried out. The experimental behaviour, stress-strain and pore pressure, have been fitted using the theoretical equations emerged from PNP in the pre and post-peak regions, and their parameters values were found. The following major findings were:

1. Stress-strain curves for the pre-peak region were fitted using the inverted function (y_I), Eq. (2), with ν=2, although in three cases ν=2.5 was found a better fit. The values σ_{eo}/σ_{co} decreases of 6.3 to 2.6 as the effective consolidation stress increase from 100 to 500 kPa. The peak friction angle values were found between 27^0 to 34^o.

2. The pore pressure coefficients values were α=1 and β between 2 and 3, although one experimental pore pressure curve (A3) were better fitted using β=4.

3. The stress-strain behaviour in the post-peak region was fitted using the ductility function (y_D) with ν=1. The deviator residual stress $(\sigma_1-\sigma_3)_\infty$ was found between 308 y 1358 kPa, with a friction residual angle between 15° to 27°, respectively.

ACKNOWLEDGMENTS

The authors of this work desire to express their ample acknowledgment to the "Dirección General de Asuntos del Personal Académico (DGAPA) of the National University of Mexico for the economic grant provided through the "Programa de Apoyo a Proyectos de Investigacion e Innovación Tecnológica (PAPIIT), proyecto IN100705.

We are also grateful for the unconditioned assistant given by the Soil Mechanics Laboratory personnel of the "División de Ingeniería Civil Topográfica y Geodésica" of the "Facultad de Ingeniería" of the National University of México.

REFERENCES

Head, K.H. (1994). *Manual of soil laboratory testing*, Volume 1, 2 and 3, Pentech Press, London.

Jerónimo-Rodríguez, F. (2003). The Principle of Natural Proportionality applied to describe the stress-strain behaviour for sands subjected to triaxial compression tests on drained and undrained conditions, *Master Thesis*, PPI, UNAM, México (in Spanish).

Juárez-Badillo, E. (1985). General volumetric constitutive equation for geomateriales, Special volume on Constitutive Laws of Soils, *XI International Conference on Soil Mechanics and Foundations Engineering*, San Francisco, USA., *Japanese Society for Soil Mechanics and Foundations Engineering*, Tokyo: 131-135.

Juárez-Badillo, E. (1997). General equations to describe the mechanical behaviour of granular soils, *XIV Interantional Conference on Soil Mechanics and Foundation Engineering*, Hamburg, Germany, Vol. 1: 133-138.

Juárez-Badillo, E. (1999a). Static liquefaction of very lose sands: Discussion *, Canadian Geotechnical Journal*, Vol. 36: 967-973.

Juárez-Badillo, E. (1999b). Static liquefaction of sands under multiaxial loading: Discussion, *Canadian Geotechnical Journal*, Vol. 36: 974-979.

Juárez-Badillo, E. (1999c). Improved general stress-strain equations for granular soils*, XI Panamerican Conference on Soil Mechanics and Foundation Engineering*, Foz do Iguassu, Brazil, Vol. 1: 297-306.

McManus, K.J. and Davis, R.O. (1997). Dilation-induced pore fluid cavitation in sands*, Geotechnique 47,* No. 1, 173-177.

Ovando, S. E. (1985). Stress-strain behaviour of granular soils tested en the triaxial cell, *PhD Thesis*, School of Engineering, Imperial College of Science and Technology.